gaps. They have the capability to image not only through clouds, but also during the darkness of antarctic winters, and they could provide complete coverage in the immediate vicinity of the poles. Several such missions are in the planning stages (*2*).

Overall, the space-borne imaging systems that have now acquired images of Antarctica since the early 1970's, and their successors that will fly repeatedly in the future, offer a unique opportunity to measure the velocity of outlet glaciers and ice streams of the polar ice sheets quickly and inexpensively. These systems will enable us to obtain data that are essential for calculating discharge rates, and, in turn, for monitoring the mass balance of the ice sheets, ultimately helping to monitor associated changes in the world climate.

REFERENCES

1. C. W. M. Swithinbank, *Geogr. Ann. Ser. A* **65**, 289 (1983).
2. R. H. Thomas *et al.*, *NASA Tech. Memo. 86233* (1985).
3. S. D. Hicks, *J. Geophys. Res.* **83**, 1377 (1978).
4. B. K. Lucchitta, E. M. Eliason, C. S. Southworth, *Antarct. J. U.S.* **19**, 249 (1983).
5. B. K. Lucchitta, J. A. Bowell, K. E. Edwards, E. M. Eliason, H. M. Ferguson, *U.S. Geol. Surv. Bull.*, in press.
6. T. Hughes, *Rev. Geophys. Space Phys.* **15**, 1 (1977).
7. C. W. M. Swithinbank and B. K. Lucchitta, *Ann. Glaciol.* **8**, 159 (1986).
8. O. Orheim and B. K. Lucchitta, *ibid.*, in press.
9. C. W. M. Swithinbank, *Science* **141**, 523 (1963).
10. M. Giovinetto, E. S. Robinson, C. W. M. Swithinbank, *J. Glaciol.* **6**, 55 (1964).
11. T. Hughes and J. L. Fastook, *Antarct. J. U.S.* **16**, 86 (1981).
12. H. H. Brecher, *ibid.* **17**, 79 (1982).
13. I. Allison, *J. Glaciol.* **22**, 223 (1979).
14. W. R. MacDonald, *U.S. Geol. Surv. Prof. Pap. 929* (1976), p. 37.
15. R. S. Williams, Jr., J. G. Ferrigno, T. M. Kent, J. R. Schoonmaker, *Ann. Glaciol.* **3**, 321 (1982).
16. D. Lindstrom and D. Tyler, *Antarct. J. U.S.* **19**, 53 (1985).
17. R. B. Southard and W. R. MacDonald, *J. Res. U.S. Geol. Surv.* **2**, 385 (1974).
18. W. R. MacDonald, *U.S. Geol. Surv. Prof. Pap. 929* (1976), p. 194.
19. R. S. Williams, Jr., J. Ferrigno, T. M. Kent, *U.S. Geol. Surv. Open-File Report 84-573*, two sheets, 1:5,000,000 scale map (1984).

16 June 1986; accepted 19 August 1986

Three-Dimensional Structure of Favin: Saccharide Binding–Cyclic Permutation in Leguminous Lectins

GEORGE N. REEKE, JR., AND JOSEPH W. BECKER

The three-dimensional structure of favin, the glucose- and mannose-binding lectin of *Vicia faba* (vetch, broad bean), has been determined at a resolution of 2.8 angstroms by molecular replacement. The crystals contain specifically bound glucose and provide the first high-resolution view of specific saccharide binding in a leguminous lectin. The structure is similar to those of concanavalin A (Con A) and green pea lectin; differences from Con A show that minimal changes are needed to accommodate the cyclic permutation in amino acid sequence between the two molecules. The molecule is an ellipsoidal dimer dominated by extensive β structures. Each protomer contains binding sites for two divalent metal ions (Mn^{2+} and Ca^{2+}) and a specific saccharide. Glucose is bound by favin in a cleft in the molecular surface and has noncovalent contacts primarily with two peptide loops, one of which contains several metal ion ligands. The specific carbohydrate-binding site is similar to that of Con A in location and general peptide folding, despite several differences in specific amino acid residues.

LECTINS INCLUDE A WIDE ASSORTMENT of proteins from various sources and have the common property of binding specific saccharides (*1, 2*). Although their natural functions are unknown in most cases, and undoubtedly differ among the different classes of lectins, these proteins are highly useful reagents in biochemistry and cell biology. They have been used, among other things, for labeling and studying the dynamics of cell surfaces, for stimulating mitosis in lymphocytes and other cells, and as affinity reagents for isolating glycopeptides and glycoproteins.

Extensive amino acid sequence homologies among the lectins of the Leguminosae suggest a common evolutionary origin for these proteins (*3, 4*). Each of them has protomers of approximately 230 amino acid residues that contain binding sites for Mn^{2+}, Ca^{2+}, and a specific carbohydrate. The protomers can be divided into three subclasses (*5*). The first includes concanavalin A (Con A), the lectin of *Canavalia ensiformis*, which is a tetramer of four identical 237-residue chains. The second includes the glucose- and mannose-binding lectins from *Vicia faba*, *Lens culinaris*, *Pisum sativum*, *Vicia sativa*, and *Vicia cracca*. These proteins are dimers, the subunits of which are composed of an α chain (M_r = 5600) and a β chain (M_r = 20,000), which together are equivalent to a Con A monomer. Comparison of the primary structures of these proteins with Con A reveals an unusual circular permutation of extensive homologous sequences (*6, 7*). In the case of favin, the β chain (residues 1 to 182) homology begins at residue 120 of Con A and extends to the carboxyl terminus of that molecule. It continues without interruption through the amino terminal 69 residues of Con A. The α chain of favin (residues 183 to 233) maintains the continuous homology through the remaining 50 residues (70 to 119) of Con A. The proteins of the third subclass, which includes the lectins from soybeans, peanuts, red kidney beans, and the GalNAc-binding lectins from *V. cracca* and *Dolichos biflorus*, are composed of single chains similar in size to the Con A monomer, but they too are circularly permuted, being equivalent to covalently joined α and β chains of the second subclass. It has been shown recently that these different subclasses arise as a result of different posttranslational modifications of similar precursor molecules which consist of a soybean-type sequence preceded by a signal sequence. In the processing of favin, the signal sequence is removed, a carbohydrate moiety is covalently attached to Asn 168, and the remaining chain is cleaved to produce the mature α and β chains (*8*). The processing of Con A is quite unusual: the signal peptide is removed, the chain is cleaved into smaller chains and then reannealed to produce the circularly permuted sequence expressed in the mature protein (*9*).

Of these lectins, three-dimensional structures have been determined only for Con A (*10–12*) and pea lectin (*13, 14*). Although the saccharide-binding site in Con A has been located by means of heavy atom–labeled carbohydrates at low to medium resolution (*15, 16*), none of the known structures has included bound, unlabeled saccharide at high resolution. We now report the crystallographic determination at a resolution of 2.8 Å of the structure of favin. This study allows us to compare the chain foldings of permuted sequences from two different subclasses. In addition, crystals of favin were grown in the presence of glucose, providing the first opportunity to examine the specific carbohydrate-protein binding interactions of a leguminous lectin at high resolution.

The asymmetric unit of favin crystals (*17*) contains a complete dimeric molecule (M_r = 51,000) comprising two α chains, two β

Department of Developmental and Molecular Biology, Rockefeller University, New York, NY 10021.

chains with covalently bound carbohydrate, and two noncovalently bound glucose molecules. X-ray diffraction data were collected by precession and oscillation photography to 2.8-Å spacings, the limit of useful resolution afforded by the crystals. Attempts to prepare isomorphous heavy atom derivatives were unsuccessful. The structure was solved by molecular replacement methods based on atomic coordinates for pea lectin (*18*). Rotation functions (*19*) were calculated from a model structure consisting of 95% of a complete pea lectin dimer: the polypeptide backbone, all side chains identical in the two molecules, and the two metal ions. Data with Bragg spacings between 20 and 6 Å were used with a radius of integration of 35 Å. These rotation functions revealed two alignments of high significance related by a rotation of 180°, corresponding to the two possible alignments between dimers of pea lectin and favin. T1 translation functions (*20*) were calculated for both rotations from data obtained at resolutions between 4 and 8 Å. These functions produced equivalent models of the favin structure. The six alignment parameters were refined by rigid body least-squares refinement (*21*). A Sim-weighted (*22*) difference electron density map was calculated with coefficients $[2k|F_o| - |F_c|]\exp(i\alpha_c)$ (where $|F_o|$ is the observed structure factor magnitude, $|F_c|$ is the calculated structure factor magnitude, α_c is the calculated phase, and k is a scale factor to put observed data on the absolute scale) and phases derived from the transformed coordinates of the pea lectin model described above.

The features of this map suggested strongly that it was not overly biased by the molecular replacement model. Several features of favin that are not in the pea lectin model are visible in both crystallographically independent protomers, including the COOH-terminal Pro-Leu residues of the two β chains and the specifically bound glucose molecule. Over 30 Å away from the specifically bound glucose, two rings of the carbohydrate moiety that is covalently attached to Asn 168 in each protomer are also visible. The remaining parts of these groups are apparently disordered in the crystals, perhaps because of their known chemical heterogeneity (*23, 24*). In addition, where the amino acid sequences of pea lectin and favin differ, the electron density map is consistent with the favin sequence. One residue at the NH_2-terminus and four at the COOH-terminus are not visible, presumably because of crystallographic disorder. We derived atomic coordinates for favin by fitting the amino acid sequence (*6*) to this map by means of a computer graphics model-building program (*25*). These coordinates

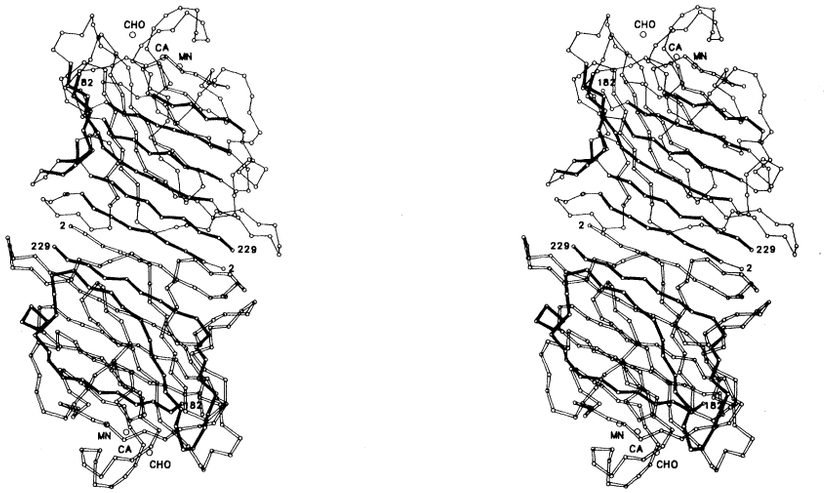

Fig. 1. Stereoscopic α-carbon representation of the favin dimer viewed down the noncrystallographic twofold axis. In the upper protomer, residues involved in the front β structure are connected with double-line bonds and those involved in the back β structure are connected with heavy solid bonds. In the lower protomer, the α chain is emphasized. Sites for Mn^{2+} (MN), Ca^{2+} (CA), and saccharide (CHO) are indicated by the larger circles near the top and bottom of the drawing.

were subjected to preliminary restrained least-squares refinement (*21*). At present, the standard crystallographic R factor for 10,275 observed reflections is 0.38, and the root-mean-square deviation of all bond lengths from standard values is 0.020 Å. The appearance of $2F_o - F_c$ and $F_o - F_c$ maps based on the phases of the refined structure is excellent, but it suggests that further fitting and refinement will improve the interpretation in certain regions of the structure. All computations for which explicit references have not been given were performed with the ROCKS system of programs (*26*).

The structure of favin is, in general, very similar to those of Con A and the pea lectin. There are several detailed differences, particularly with Con A, that are consistent with differences in carbohydrate-binding specificity and quaternary structure. The favin dimer (Fig. 1) is composed of two crystallographically distinct subunits related by a local twofold symmetry axis. The subunits, like those of Con A and pea lectin, are folded into compact dome-shaped structures approximately 42 by 40 by 39 Å in size. The two subunits are very similar: after rotation of one subunit about the local twofold axis, corresponding α-carbons superimpose to within a root-mean-square difference of 0.48 Å.

The secondary structure of the protomer is dominated by two large antiparallel β structures that are, except for the circular permutation of sequence, identical in arrangement and connectivity to those of Con A. One of these, comprising six strands, forms the rear of the molecule as seen in Fig. 1 (top). Beginning at the fourth strand from the top, a portion of this sheet is bent sharply forward to form the left surface of the molecule. The bottom strand of this same sheet is hydrogen-bonded to its sym-

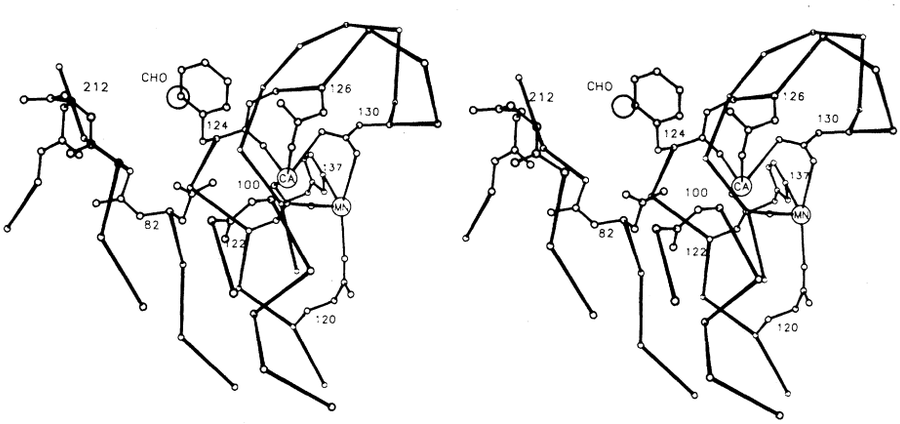

Fig. 2. Closeup stereo view of the region of metal ion and saccharide binding in favin. The Mn^{2+} and Ca^{2+} ions are at the top right; the *cis*-linked Ala 81–Asp 82 peptide at lower center; and the saccharide at the left. Residues implicated in specific interactions with the bound saccharide are listed in the text.

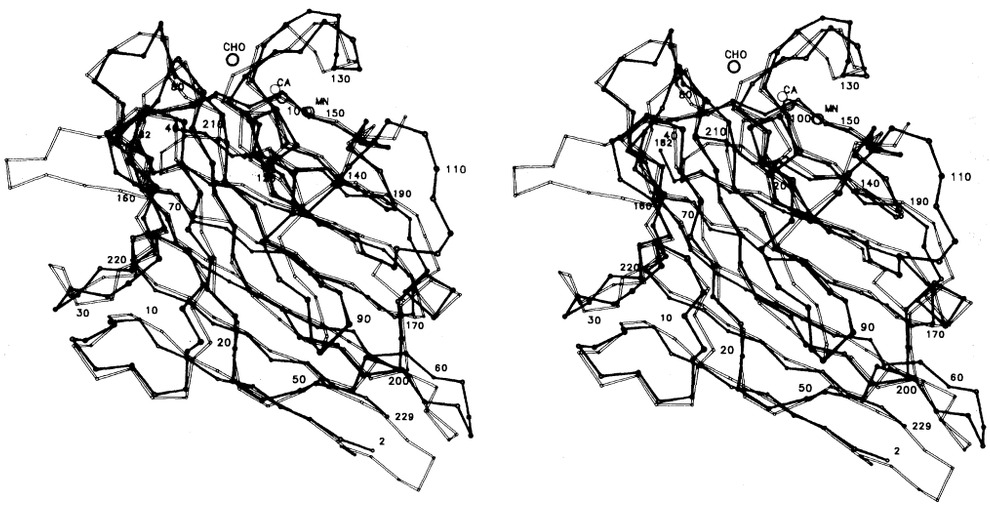

Fig. 3. Stereo diagram showing superimposed monomers of favin (heavy lines) and Con A (light lines) in the same orientation as Fig. 1. The different locations of the ends of the Con A and the two favin polypeptide chains are discussed in the text; all can be seen to be located on the surface of the molecule, away from the region of metal and saccharide binding and near to stabilizing secondary structural features.

metry-related counterpart in the other monomer to form a single 12-stranded sheet running across the entire back surface of the dimer. The second β structure, which contains seven strands, twists through the central part of the subunit and contains many of the residues involved in metal and saccharide binding, as discussed below. The α and β chains are intimately interwoven in the complete structure (the α chain forms the second and fifth strands of the rear pleated sheet and the fifth strand of the central sheet; Fig. 1, bottom) and it appears that the folding pattern of neither chain could be stable in the absence of the other. The two chains together, like the single chain of Con A (*10*), thus form a single domain.

Divalent metal ions and specific saccharides are bound in a complex and interconnected group of sites (Fig. 2). In favin, pea lectin, and Con A, the polypeptide chain folding is generally conserved in this region; the amino acid sequences are conserved in the metal-binding sites, but not the carbohydrate-binding sites, consistent with their specificity. As in Con A, Mn^{2+} and Ca^{2+} are bound in a double site with two protein ligands binding to both metals. The direct side-chain ligands (Glu 120, Asp 122, Asp 130, and His 137 to Mn^{2+}; Asp 122, Asn 126, and Asp 130 to Ca^{2+}) are the same in both proteins. The backbone carbonyl oxygen of Phe 124 is a Ca^{2+} ligand in favin; the homologous ligand in Con A is the carbonyl oxygen of a tyrosine. As in Con A, the Mn^{2+} coordination is completed by two water molecules that are apparently hydrogen-bonded to the carbonyl oxygen of Ile 145 (Ser 32 in Con A) and the hydroxyl oxygen of Ser 147 (Ser 34 in Con A). Also as in Con A, Ca^{2+} has two water ligands, one of which is hydrogen bonded to the side chain of Asp 82 (Asp 208 in Con A). This group also forms part of the carbohydrate-binding site, and it is adjacent to an unusual *cis* peptide linkage (Ala 81–Asp 82) that is present in all three lectins.

The stereospecifically bound glucose appears as a peak of electron density in both subunits in both $2F_o - F_c$ and $F_o - F_c$ maps. The saccharide is bound in a cleft in the protein surface between the loop of peptide enclosing the metal sites, chains extending from the front β structures, and a loop including residues 99 and 100. This site is analogous to that found in Con A (*15, 16*). Although the glucose electron density is strong and of the appropriate size, its shape at the present stage of refinement is poorly defined, and it is not possible to orient a model within it unambiguously. Polar groups that are in position to interact with carbohydrate include the main chain nitrogens of Gly 100, Ala 212, and Thr 213, the side chains of Asn 40 and Asn 126, and the side chain of the *cis*-linked Asp 82. This Asp residue is hydrogen-bonded to a water molecule that is one of the Ca^{2+} ligands, and stabilization of the *cis* peptide linkage by Ca^{2+} is thought to be a major element in the induction of the active, saccharide-binding state of the lectin on addition of metals (*27, 28*). The major structural difference between Con A and favin in this region is the replacement of two large side chains, Leu 99 and Arg 228 in Con A, with smaller groups, Ala 212 and Gly 100, in favin. These replacements make the favin site considerably more open than that of Con A and may account for the fact that substitution of methyl or phenyl groups at O3 enhances carbohydrate binding by favin, but decreases it in Con A.

Although the polypeptide folding of the favin protomer is similar to that of Con A (Fig. 3), the localization of amino acid sequence differences within the three-dimensional structure is consistent with the observed differences in quaternary structure. When the two structures are aligned by least-squares rigid-body methods, the root-mean-square distance between 217 corresponding α-carbons is only 1.4 Å. The largest difference in folding is a loop of seven residues near residue 160 in the Con A sequence that is not present in the analogous region of favin, near residue 36. The different chain structures account for the remaining prominent differences: the loop of peptide containing favin residues 108 to 115 that corresponds to the gap between the COOH- and NH_2-termini of Con A; the reverse turn near residue 120 of Con A that is aligned with the NH_2-terminus of the favin β chain and the COOH-terminus of the α chain; and the cleaved bond between favin residues 182 and 183, corresponding to a β bend at residues 67 to 70 of Con A. A further significant difference is that most of the amino acid side chains (35 out of 44 residues) projecting from the rear of the back β structure are different in the two lectins. It is through these groups that two Con A dimers interact to form a tetramer, an interaction that does not occur in favin. Examination of the structures indicates that none of the residues involved in electrostatic bonds between the two Con A dimers is charged in favin, removing a major possible source of stabilization for further interactions. In addition, the covalently attached saccharide of favin is contained in this region, possibly hindering tetramerization by its bulk.

The similarity in three-dimensional structure, together with studies on the synthesis and posttranslational processing of favin (*8*) and Con A (*9*), suggests strongly that both molecules are synthesized as precursors of similar structure and that the different modes of posttranslational processing, which produce the observed circular permutation of sequence, occur without major structural rearrangements. Two additional observations support this hypothesis: first, the sites of posttranslational processing are

all at the molecular surface where they would be accessible to enzymes without any significant structural rearrangement, and second, at each of these sites (near favin residues 1, 110, and 182) the structures of favin and Con A differ only slightly and the differences are highly localized. Both molecules are apparently synthesized as precursors similar in three-dimensional structure to favin, but with a signal sequence at the NH_2-terminus and with residues 182 and 183 in favin joined by a peptide bond and local conformation similar to that between residues 69 and 70 in Con A.

In conclusion, the comparison of the superimposed molecules suggests that the differing biosynthetic patterns of the two molecules are of minimal significance for the function of the monomers. In all cases, peptide links that are missing in one or the other of the two proteins are located well away from the region of metal and saccharide binding and near to secondary structural features that would be expected to stabilize the structure near the "frayed ends" introduced by the various cleavages. The key features of the metal-binding region are nearly the same in the two structures, and the differences that are seen in the saccharide-binding region can be related to the differences in binding specificity of the two proteins. Further crystallographic refinement now in progress should provide a detailed picture of these interactions.

REFERENCES AND NOTES

1. H. Lis and N. Sharon, *Annu. Rev. Biochem.* **55**, 35 (1986).
2. M. E. Etzler, *Annu. Rev. Plant Physiol.* **36**, 209 (1985).
3. A. Foriers, C. Wuilmart, N. Sharon, A. D. Strosberg, *Biochem. Biophys. Res. Commun.* **75**, 980 (1977).
4. J. J. Hemperly and B. A. Cunningham, *Trends Biochem. Sci.* **8**, 100 (1983).
5. J. W. Becker, B. A. Cunningham, J. J. Hemperly, in *Chemical Taxonomy, Molecular Biology and Function of Plant Lectins*, I. J. Goldstein and M. E. Etzler, Eds. (Liss, New York, 1983), pp. 31–45.
6. B. A. Cunningham, J. J. Hemperly, T. P. Hopp, G. M. Edelman, *Proc. Natl. Acad. Sci. U.S.A.* **76**, 3218 (1979).
7. A. Foriers, E. Lebrun, R. Van Rapenbusch, R. deNeve, A. D. Strosberg, *J. Biol. Chem.* **256**, 5550 (1981).
8. J. J. Hemperly, K. E. Mostov, B. A. Cunningham, *ibid.* **257**, 7903 (1982).
9. D. J. Bowles *et al.*, *J. Cell Biol.* **102**, 1284 (1986).
10. J. W. Becker, G. N. Reeke, Jr., J. L. Wang, B. A. Cunningham, G. M. Edelman, *J. Biol. Chem.* **250**, 1513 (1975).
11. G. N. Reeke, Jr., J. W. Becker, G. M. Edelman, *ibid.*, p. 1525.
12. K. D. Hardman and C. F. Ainsworth, *Biochemistry* **11**, 4910 (1972).
13. E. J. Meehan, Jr., J. McDuffie, H. Einspahr, C. E. Bugg, F. L. Suddath, *J. Biol. Chem.* **257**, 13278 (1982).
14. R. R. Riskulov *et al.*, *FEBS Lett.* **165**, 97 (1984).
15. J. W. Becker, G. N. Reeke, Jr., G. M. Edelman, *Nature (London)* **259**, 406 (1976).
16. K. D. Hardman and C. F. Ainsworth, *Biochemistry* **15**, 1120 (1976).
17. J. L. Wang, J. W. Becker, G. N. Reeke, Jr., G. M. Edelman, *J. Mol. Biol.* **88**, 259 (1974).
18. H. Einspahr, E. H. Parks, K. Suguna, E. Subramanian, F. L. Suddath, *J. Biol. Chem.*, in press.
19. R. A. Crowther, in *The Molecular Replacement Method*, M. G. Rossmann, Ed. (Gordon and Breach, New York, 1972), pp. 173–185.
20. R. A. Crowther and D. M. Blow, *Acta Crystallogr.* **23**, 544 (1967).
21. W. A. Hendrickson and J. H. Konnert, in *Computing in Crystallography*, R. Diamond, S. Rameseshan, K. Venkatesan, Eds. (Indian Academy of Sciences, Bangalore, 1980), pp. 13.01–13.23.
22. G. A. Sim, *Acta Crystallogr.* **13**, 511 (1960).
23. A. N. Allen, N. N. Desai, A. Neuberger, *Biochem. J.* **155**, 127 (1976).
24. T. P. Hopp, J. J. Hemperly, B. A. Cunningham, *J. Biol. Chem.* **257**, 4473 (1982).
25. A. Jones, *J. Appl. Crystallogr.* **11**, 268 (1978).
26. G. N. Reeke, Jr., *ibid.* **17**, 125 (1984).
27. G. N. Reeke, Jr., J. W. Becker, G. M. Edelman, *Proc. Natl. Acad. Sci. U.S.A.* **75**, 2286 (1978).
28. R. D. Brown, C. F. Brewer, S. H. Koenig, *Biochemistry* **16**, 3883 (1977).

29. We thank F. L. Suddath and his colleagues for making available their coordinates for pea lectin in advance of publication. We also thank A. R. Fraser, J. J. Hemperly, and W. E. Gall for their contributions to earlier stages of this project, and especially G. M. Edelman and B. A. Cunningham for their advice and encouragement. Technical assistance was provided by S. Marglin. Atomic coordinates will be deposited with the Protein Data Bank upon completion of the crystallographic refinement now in progress. This work was supported by USPHS grant AI-11378, NSF grant PCM7709377, and development of computer programs by USPHS grant GM-22663.

16 July 1986; accepted 23 September 1986

Reversible Interconversion of Two Forms of a Valyl-tRNA Synthetase–Containing Protein Complex

SIMON BLACK

When an enzyme-containing complex from yeast was incubated in a buffered solution at room temperature, the valyl–transfer RNA synthetase activity and total protein oscillated synchronously between two physical states. This observation suggests a regulatory process that controls a number of enzymes as a group, an integrated function of a kind not heretofore recognized. The two forms of the complex were separated by ammonium sulfate precipitation of one of them in samples withdrawn from the incubated solution every 30 seconds. Glutathione and dithiothreitol in high concentrations (50 m*M*) enhance formation of the 50% saturated ammonium sulfate–soluble form. Oxidized glutathione, diphosphopyridine nucleotide, triphosphopyridine nucleotide, and a mercurial thiol binding agent in moderate concentrations (0.1 to 1.0 m*M*) shift the distribution toward the precipitable form. It is suggested that the two forms represent functional and nonfunctional complex-bound enzymes which are interconverted in response to oxidoreductive signals.

THE HYPOTHESIS THAT THE THIOL and disulfide groups on the surfaces of many enzyme molecules participate in the regulation of catalytic rates has a long history (*1*) and is well supported for certain photosynthetic systems (*2*). Evidence that these groups may participate in regulating the first step of protein biosynthesis, the aminoacylation of transfer RNA (tRNA), is provided by a valyl-tRNA synthetase-containing complex (*3, 4*). The synthetase requires a thiol for an activation process that is blocked by arsenite, which is a strong binder of pairs of adjacent thiol groups (*3*). It has now been found that when the complex is incubated in a buffered solution at room temperature, at a concentration about 100-fold greater than is used in enzyme activity tests, a rapid oscillatory change in state occurs that is affected by oxidoreductive and thiol-reactive agents. The change in state is evident from a change in the solubility of the complex in 50% saturated ammonium sulfate. These findings suggest a new function for the thiol group in a novel synchronous regulation of several enzymes associated in a complex.

The unstable complex used in the experiments was prepared from concentrated yeast cell sap (*3*), and would probably not survive the dilution accompanying more conventional procedures for isolating enzymes.

In the first experiment, the enzyme activities alternated between the supernatant and precipitate fractions (Fig. 1A), and total protein behaved similarly (Fig. 1B). Arsenite, which was present in this experiment, was assumed to be oxidoreductively neutral in the test environment. When arsenite was omitted, the oscillation was faster but deteriorated rapidly after 1 to 3 minutes. In 50 m*M* inorganic sulfide (Fig. 2), the most rapid oscillation was too fast to be adequately characterized with the present procedure, but well-defined cycles were evident between 3.5 and 8.5 minutes. In the presence of thiols (1.0 to 10 m*M*) or inorganic sulfide (5 to 50 m*M*), oscillatory interconversion continued for several hours, after which 80 to 90% of the enzyme activity and 60 to

Section on Pharmacology, Laboratory of Biochemical Pharmacology, National Institute of Diabetes and Digestive and Kidney Diseases, Bethesda, MD 20892.